JOURNAL OF SOLID STATE CHEMISTRY **84**, 237–244 (1990)

The Crystal and Magnetic Structures of $Sr_2LaFe_3O_8$

P. D. BATTLE,* T. C. GIBB, AND P. LIGHTFOOT

School of Chemistry, The University of Leeds, Leeds, LS2 9JT, England

Received May 30, 1989; in revised form September 28, 1989

The crystal and magnetic structures of the anion-deficient perovskite $Sr_2LaFe_3O_8$ (space group *Pmma*, $a = 5.5095(1)$, $b = 11.8845(5)$, $c = 5.6028(1)$ Å) have been refined from X-ray and neutron powder diffraction data collected at room temperature. The crystal structure consists of layers of octahedral (O) and tetrahedral (T) iron–oxygen polyhedra arranged in the stacking sequence . . .OOTOOT. . . perpendicular to the $\hat{y}$ axis of the unit cell. The magnetic structure is that of a G-type antiferromagnet with ordered magnetic moments of 3.77(5) and 3.15(11) μ_B at the octahedral and tetrahedral sites, respectively. The low moment at the tetrahedral site is consistent with the observed disorder and magnetic anisotropy.

Introduction

In a recent paper (*1*) we reported the preparation of an ordered-vacancy perovskite phase, $Sr_2LaFe_3O_8$, and its characterization by X-ray powder diffraction and Mössbauer spectroscopy. The compound was shown to be structurally related to $Ca_2LaFe_3O_8$, which was first prepared by Grenier *et al.* (*2, 3*) as one of a series of orthorhombic perovskite-related phases (unit cell $\sqrt{2}a_p \times 3a_p \times \sqrt{2}a_p$) of general formula $Ca_2Fe_2O_5 \cdot ABO_3$ (A = Ca, Sr, Ba, B = Ti; A = Y, La, Gd, B = Fe). These could be described as representing the $n = 3$ member in a series $A_nB_nO_{3n-1}$, where $n = 2$ is the $A_2B_2O_5$ brownmillerite and $n = \infty$ is the ABO_3 perovskite structure. The oxygen vacancies are ordered along the [101] directions of the cubic perovskite cell such that layers of B cations in octahedral and tetrahedral coordination are formed perpendicular to the [010] axis of the aristotype cell, giving rise to the layer sequences OTOT′ . . . in $A_2B_2O_5$ (Fig. 1) and OOTOOT. . . in $A_3B_3O_8$. Note that there are two orientations (T and T') for the tetrahedra in brownmillerite, but available evidence indicates that there is normally only one orientation in $A_3B_3O_8$. The occurrence of the OOT sequence in $Ca_2LaFe_3O_8$ has been verified (*4*) by transmission electron microscopy, although a full crystal structure has never been obtained, possibly because of the stacking disorder which may occur along the *b*-axis.

A similar OOT stacking sequence has been reported (*5*) in the $CaFe_{1-x}Mn_xO_{3-y}$ system, and a partial structure refinement was obtained from X-ray powder data. However, manganese is known to favor a square-based pyramidal coordination in oxygen-deficient perovskites, and hence it may well be that this phase is quite different from those which contain iron as the only transition metal. A very recent report (*6*)

---

* To whom correspondence should be addressed.

0022-4596/90 $3.00

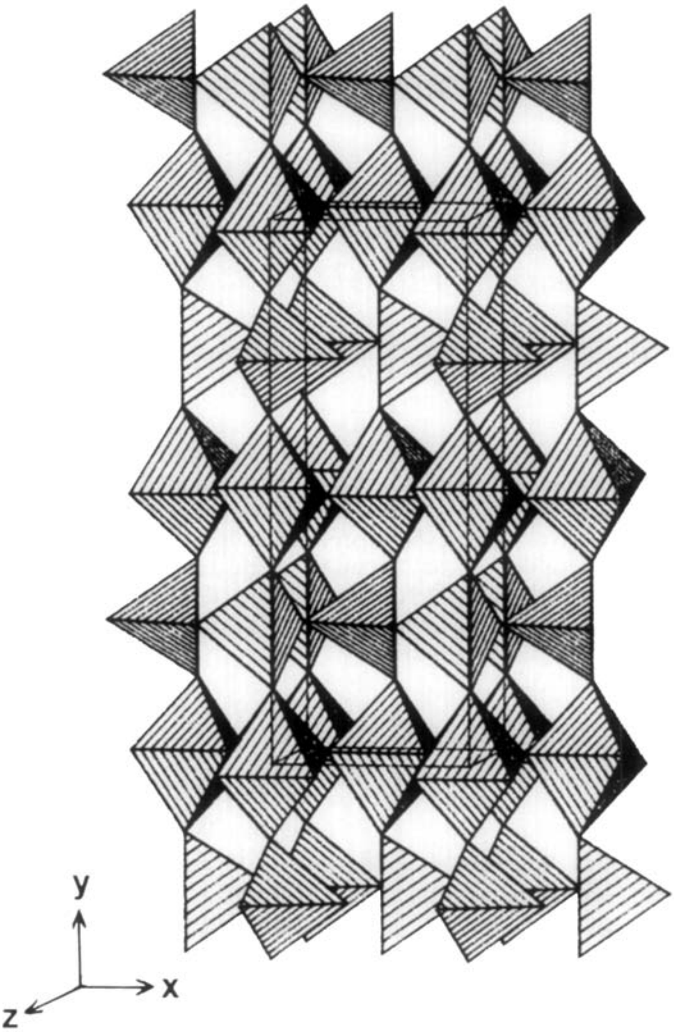

FIG. 1. The transition metal polyhedra in the brownmillerite structure.

describes an additional X-ray investigation of $Ca_3(Fe, Mn)_3O_8$ and also of $Ca_3Fe_2TiO_8$, but again the use of X-rays leads to a poorly defined structure.

In this paper we report a detailed crystallographic and magnetic structural characterization of $Sr_2LaFe_3O_8$ using synchrotron X-ray powder diffraction and neutron diffraction techniques. This is the most detailed structure to be obtained for the OOT stacking sequence to date, and provides a new insight into its relationship to the brownmillerite structure.

Experimental

The preparation of $Sr_2LaFe_3O_8$ has been described elsewhere (*1*). The sample used for the synchrotron X-ray measurements was that used earlier for the detailed characterization by Mössbauer spectroscopy. The reddish-brown material was obtained with a final anneal at 1000°C *in vacuo* ($<10^{-4}$ Torr). The larger sample used for the neutron measurements was prepared in a similar manner, with the final anneal at 950°C *in vacuo*.

X-ray powder diffraction data were collected on the powder diffractometer 8.3 at the Synchrotron Radiation Source, Daresbury. The angular range $5 < 2\theta < 94°$ was scanned in steps of 0.01° with the instrument operating in flat-plate geometry at a wavelength of 1.5084 Å. Neutron powder diffraction data were collected at room temperature on the powder diffractometer D1a at ILL Grenoble. The angular range $0 < 2\theta < 156°$ was scanned in steps of 0.05° using a wavelength of 1.909 Å. Approximately 10 g of sample were contained in a vanadium can of diameter 12 mm during the data collection, which took ca. 11 hr.

Results

The X-ray diffraction pattern of our sample of $Sr_2LaFe_3O_8$ could be indexed in an orthorhombic unit cell having a = 5.5095(1), b = 11.8845(5), c = 5.6028(1) Å and space group *Pmma,* Pm2*a*, or *P*2$_1$*ma*. We began our data analysis in the centrosymmetric group *Pmma*. In this unit cell and space group, the cation arrangement in the perovskite-related structure described above consists of two crystallographically distinct sites for the *A*-site cations (initially taken to be a fully disordered arrangement of Sr and La), one Fe^{3+} site (Fe1) in octahedral coordination to oxygen, and one Fe^{3+} site (Fe2) in tetrahedral coordination to oxygen. The anion sublattice contains three oxide ions (O1, O2, and O3) which are arranged only around the six-coordinate cations, one oxide ion (O4) which provides the link between the octahedral layers and the tetrahedral layers, and one oxide ion (O5) which is coordinated only to the tetrahedral Fe2 site.

Initial profile analysis of the X-ray diffraction data was carried out using the Rietveld program (*7*) as modified by Fitch *et al.* (*8*). This enabled us to refine the positions of the metal atoms, and most importantly, it provided clear evidence that the four-coordinate Fe2 cations are disordered from their ideal 2*e* ($\frac{1}{4}$, 0, z) sites in this structure. We were unable to obtain a satisfactory refinement of the oxide ions around Fe2 using the X-ray data, but we emphasize the important role that these data played in determining the course of the subsequent structure analysis. $Sr_2LaFe_3O_8$ is magnetically ordered at room temperature and, as will be described below, our neutron data therefore contain a mixture of nuclear and magnetic scattering. The availability of an X-ray data set, free of magnetic scattering, made the task of defining the cation sublattice of this compound relatively straightforward.

The coordinates from the best X-ray refinement were used as the initial parameters in the analysis of the neutron diffraction data. These data contained additional peaks which could be indexed in a unit cell doubled along $\hat{y}$. They are due to the magnetic scattering referred to above. The positions of the peaks indicted that $Sr_2LaFe_3O_8$ orders as a G-type antiferromagnet with the cation magnetic moments aligned along the crystallographic $\hat{x}$-axis. In this magnetic structure, each Fe^{3+} ion is coupled antiferromagnetically to the six nearest-neighbor cations, irrespective of whether they occupy octahedral or tetrahedral sites. In order to account for this scattering, the ordered magnetic moments on the octahedral and tetrahdral sites were included as variable parameters in the data analysis, which was once again carried out using the Rietveld method. The Bragg peaks were assumed to have a Gaussian lineshape and the background level beneath the peaks was estimated by interpolation between regions of the profile where no reflections were observed. The free-ion form factor calculated (*9*) for Fe^{3+} was used to describe the angular dependence of the magnetic scattering and the following nuclear scattering lengths were used: $b_{Sr} = 0.69$, $b_{La} = 0.83$, $b_{Fe} = 0.95$, $b_O = 0.58 \times 10^{-14}$ m.

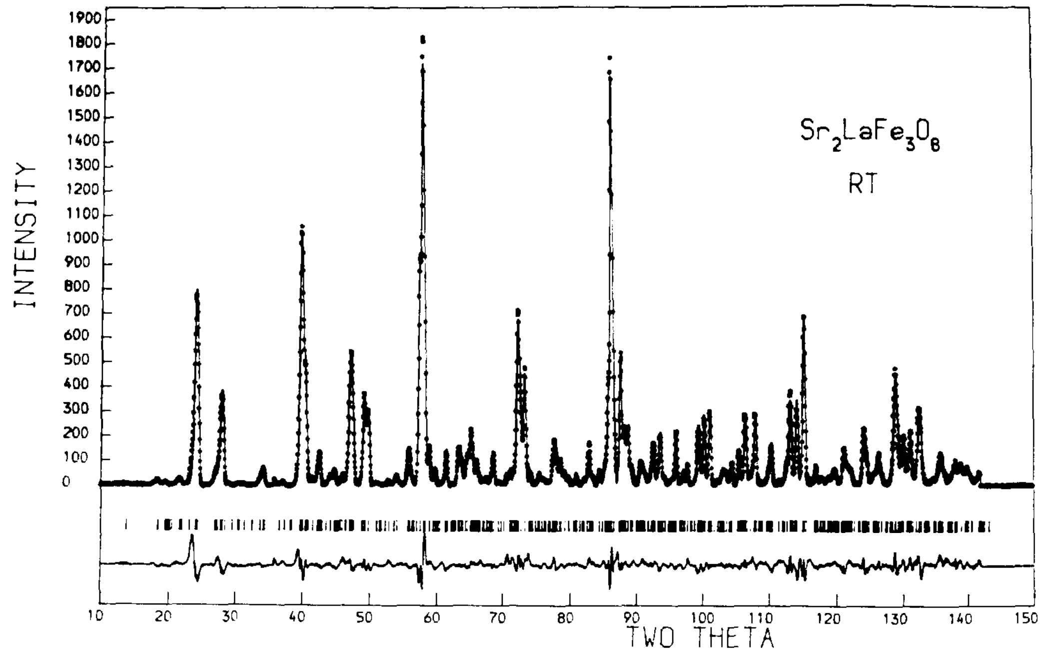

FIG. 2. Observed (...), calculated (—), and difference neutron diffraction profiles for $Sr_2LaFe_3O_8$ at room temperature.

During the initial stages of the refinement it became clear that our initial description of the anion environment around Fe2 was inadequate, and consequently we introduced disorder on the O4 and O5 sites by moving these atoms off $(\frac{1}{4}, y, z)$ and (0, 0, 0), respectively. Furthermore, in order to allow for the possible existence of T′ sites, which represent a less subtle disorder involving a reversal of the orientation of the tetrahedral site, we introduce an additional anion, O6, with the constraint that the sum of the occupation factors of O5 and O6 was constant. The final refinements included 17 atomic coordinates and two magnetic moments in addition to the usual profile parameters. It proved impossible to refine the occupation numbers of O5 and O6 and the 10 isotropic temperature factors simultaneously with the atomic coordinates and magnetic parameters, and these two sets of parameters were therefore refined alternately until minimization of the weighted profile R-factor, R_{wpr}, was achieved at a value of 12.3% (R_{exp} = 4.4%, R_I = 7.0%, R_{mag} = 16.6%). The final observed and calculated diffraction profiles and their difference are plotted in Fig. 2. The atomic parameters are tabulated in Table I and some bond lengths and bond angles are presented in Table II. Attempts to improve the agreement between the observed and calculated profiles by introducing an ordering of the strontium and lanthanum ions over the $2f$ and $4k$ sites were unsuccessful. There was no significant improvement when we refined the structure in the noncentrosymmetric space group $P2_1ma$ as an alternative to introducing disorder into the centrosymmetric group $Pmma$. The number of atoms in the asymmetric unit is the same in both space groups, but the number of variable atomic coordinates is increased to 22 when $P2_1ma$ is adopted.

TABLE I

ATOMIC PARAMETERS FOR $Sr_2LaFe_3O_8$ AT ROOM TEMPERATURE IN SPACE GROUP *Pmma*

Atom	Site	x	y	z	B_{iso} (Å)	Occupancy
Sr/La1	2*f*	$\frac{1}{4}$	$\frac{1}{2}$	0.7443(9)	0.80(7)	1
Sr/La2	4*k*	$\frac{1}{4}$	0.19114(8)	0.7307(6)	0.15(5)	1
Fe1	4*k*	$\frac{1}{4}$	0.33884(8)	0.2415(5)	0.218(8)	1
Fe2	4*i*	0.2078(8)	0	0.1786(6)	0.72(1)	$\frac{1}{2}$
O1	4*g*	0	0.3025(2)	0	0.49(7)	1
O2	4*h*	0	0.3406(2)	$\frac{1}{2}$	0.97(8)	1
O3	2*f*	$\frac{1}{4}$	$\frac{1}{2}$	0.2001(9)	0.74(10)	1
O4	8*l*	0.268(2)	0.1420(2)	0.3013(7)	1.15(8)	$\frac{1}{2}$
O5	4*i*	0.134(2)	0	0.875(2)	0.91(17)	0.46(1)
O6	4*i*	0.074(18)	0	0.688(18)	0.91(17)	0.04(1)

Note. $a = 5.5095(1)$, $b = 11.8845(5)$, and $c = 5.6028(1)$ Å. Magnetic moments: k_x (Fe1) = 3.77(5) μ_B, and k_x (Fe2) = 3.15(11) μ_B. Halfwidth parameters: $U = 2366(71)$, $V = -5314(151)$, and $W = 4531(73)$.

Discussion

The results presented above confirm the structure proposed for $Sr_2LaFe_3O_8$ on the basis of the unit-cell size and Mössbauer data. The structure, drawn in Fig. 3 (*10*), consists of double layers of corner-sharing FeO_6 octahedra, linked by single layers of FeO_4 tetrahedra. The strontium and lanthanum ions occupy the cavities between the layers. In order to discuss the structure further, it is convenient to move away from a description in terms of linked polyhedra and toward a description involving sheets of atoms stacked perpendicular to the $\hat{y}$-axis of the structure. The composition of the successive sheets is indicated in Fig. 3 and can be represented by the sequence

$$(FeO_2)(AO)(FeO_2)(AO)(FeO)(AO)$$

where A represents a disordered 2 : 1 mixture of strontium and lanthanum. The (FeO_2) layers lie within the octahedra and contain the atoms Fe1, O1, and O2. The (AO) layer between two (FeO_2) layers contains Sr/La1 and O3. The distance between Fe1 and O3 at 1.929(6) Å is the shortest iron–oxygen bond length around the octahedral site. The (AO) layer between (FeO_2) and (FeO) contains Sr/La2 and O4; Fe1–O4 at 2.365(10) Å is the longest iron–oxygen distance around the octahedral site but the $A2$–O distances are, on average, shorter than the $A1$–O distances, presumably be-

TABLE II

SELECTED BOND LENGTHS (IN Å) AND BOND ANGLES (IN DEGREES) IN $Sr_2LaFe_3O_8$ AT ROOM TEMPERATURE

Octahedral site			Tetrahedral site		
Fe1–O1	1.952(3)	(×2)	Fe2–O4	1.85(1)	(×2)
Fe1–O2	1.999(3)	(×2)	Fe2–O5	1.91(1)	
Fe1–O3	1.929(6)		Fe2–O5′	1.91(1)	
Fe1–O4	2.365(10)				
O1–Fe1–O1′	89.8		O4–Fe2–O4′	133.5	
O1–Fe1–O2	91.0	(×2)	O4–Fe2–O5	103.7	(×2)
O1–Fe1–O2′	171.8	(×2)	O4–Fe2–O5′	104.3	(×2)
O2–Fe1–O2′	87.1		O5–Fe2–O5′	108.1	
O2–Fe1–O3	94.4	(×2)			
O2–Fe1–O4	86.3				
O1–Fe1–O3	93.6	(×2)			
O1–Fe1–O4	89.0				
O4–Fe1–O1′	85.5				
O4–Fe1–O2′	83.0				
O4–Fe1–O3	177.3				
Sr/La site 1			Sr/La site 2		
Sr/La1–O1	2.968(6)	(×4)	Sr/La2–O1	2.515(4)	(×2)
Sr/La1–O2	2.713(6)	(×4)	Sr/La2–O2	2.593(4)	(×2)
Sr/La1–O3	3.049(7)		Sr/La2–O4	2.47(1)	
Sr/La1–O3′	2.554(7)		Sr/La2–O4′	2.72(1)	
Sr/La1–O3″	2.772(7)	(×2)	Sr/La2–O4″	2.92(1)	
			Sr/La2–O5	2.49(1)	

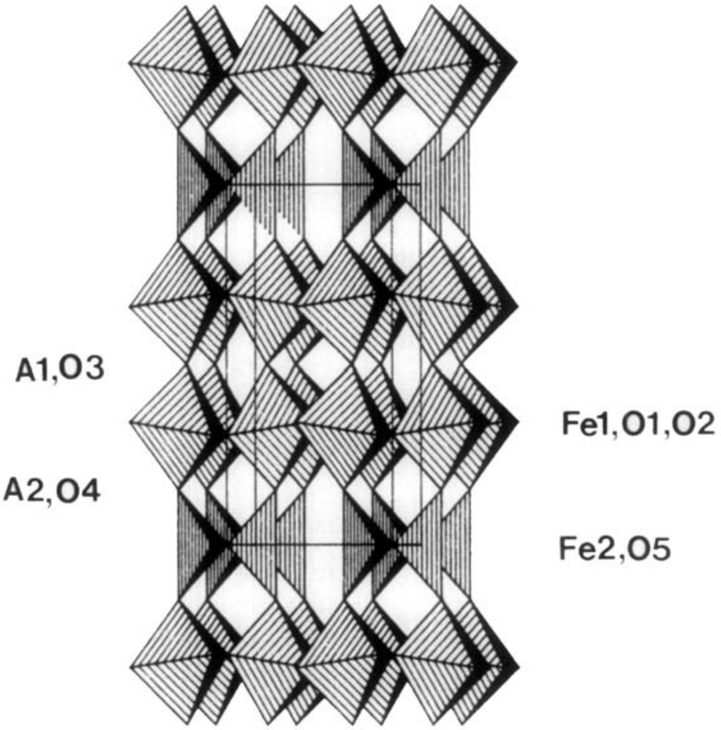

FIG. 3. The transition metal polyhedra in the structure of $Sr_2LaFe_3O_8$ drawn to emphasize the chains of anion vacancies. The long *y*-axis is in the plane of the paper.

cause *A*2 has a lower coordination number to oxygen. The (FeO) layer lies within the tetrahedra and contains Fe2 and O5; the low value for the refined occupation number of O6 suggests that, although disordered, all the FeO_4 tetrahedra in this structure have essentially the same orientation. There is no evidence to suggest that extensive intergrowth of OOTOOT and OOTOOT′ stacking sequences occurs.

There are a number of similarities between this structure and those of the brownmillerites Sr_2CoFeO_5 (*11*) and $Sr_2Fe_2O_5$ (*12*), most strikingly the observation of irregular bond angles and disorder around the tetrahedral sites, but also the existence of a long iron–oxygen distance between the octahedral and tetrahedral layers. In $Sr_2Fe_2O_5$ this distance is 2.203(2) Å compared to the four Fe–O distances in the FeO_2 layer of 1.985(1) Å. In Sr_2CoFeO_5 the distance is 2.219(4) compared to 1.969(3) Å. In $Sr_2LaFe_3O_8$ the Fe1–O4 distance of 2.365(10) Å can be compared to the mean of the four Fe–O distances in the FeO_2 layer of 1.975(3) Å; furthermore the Fe1–O3 distance which joins pairs of octahedral layers is exceptionally short at 1.929(6) Å.

In an extreme description, the structure of $Sr_2LaFe_3O_8$ could be referred to as double layers of apex-sharing FeO_5 square-based pyramids, separated by layers of FeO_4 tetrahedra. Although this description is too extreme to be appropriate, it serves to emphasize the asymmetric environment of the Fe1 cations and the relatively weak coupling between Fe1 and Fe2. The latter is reflected in the magnetic properties of the compound. Our previous Mössbauer study (*1*) showed that the temperature dependence of the internal hyperfine field at the tetrahedral site is anomalous, whereas that for the octahedral site is reasonably close to the ideal $S = \frac{5}{2}$ Brillouin function. $Sr_2LaFe_3O_8$ behaves very differently to $Sr_2Fe_2O_5$, $Ca_2Fe_2O_5$ and $Sr_2LaFe_3O_8$ despite the close similarities in the Néel temperatures of the four compounds. It was suggested (*1*) that this reflects an anisotropy in the exchange interactions which is more extreme in $Sr_2LaFe_3O_8$, and this is fully consistent with the anisotropy and disorder now revealed in the diffraction experiment. The ordered magnetic moments observed at the octahedral and tetrahedral sites, 3.77(5) and 3.15(11) μ_B, respectively, are lower than those reported (*12*) for the brownmillerite $Sr_2Fe_2O_5$ (3.98 and 4.1 μ_B, respectively) at 4.2 K. In the case of the octahedral site the difference can be explained by simple assuming that the magnetization is only 94% saturated at room temperature, this degree of saturation being consistent with our variable temperature Mössbauer data on $Sr_2LaFe_3O_8$. The latter data suggest that the magnetization at the tetrahedral site is only 86% saturated at room temperature leading to a predicted observed moment of only 3.65 μ_B for Fe2 at 4.2 K. The low observed value suggests that the structural disorder in $Sr_2LaFe_3O_8$ has a marked effect on the superexchange interactions around the tetrahedral site. We have previously suggested (*11*) that the magnetic moments of the four-coordinate cations may have components along both $\hat{x}$ and $\hat{z}$, but with only the $\hat{x}$ component showing long-range order and hence contributing to the intensities of the Bragg peaks in a neutron diffraction experiment; this model is not inconsistent with the Mössbauer data and the observed positional disorder.

There are a number of differences between the structure of $Sr_2LaFe_3O_8$ described here and that reported previously for $Ca_3Mn_{1.35}Fe_{1.65}O_{8.02}$ (*5*). The latter compound was found to have vacancies on the O3 sites, that is, at the center of the octahedral double layers, thus creating five-coordinate sites for the transition metal cations. We found no evidence for this in $Sr_2LaFe_3O_8$, consistent with the suggestion that these sites are favored by manganese cations. Nguyen *et al.* analyzed $Ca_3(Fe, Mn)_3O_8$ in the noncentrosymmetric space group *Pm*2*a* and Rodriquez-Carvajal *et al.* used $P2_1ma$, whereas we have chosen to introduce limited disorder into the centrosymmetric group *Pmma* rather than increase the number of independent structural parameters by removing the center of symmetry. We believe that this decision is justified by the level of agreement obtained between the observed and calculated intensities, and also by the magnetic behavior of the material, which is consistent with a disordered crystal structure. As stated above, there was no significant improvement in our fit when a noncentrosymmetric space group was used.

Acknowledgments

We are grateful to the SERC for the award of a postdoctoral research fellowship to P.L., for the provision of neutron scattering facilities at ILL Grenoble, where we received experimental assistance from Dr. J. K. Cockcroft, and for the provision of X-ray facilities at Daresbury where Dr. K. O.'Reilly gave assistance under the auspices of the powder diffraction service. We also thank Dr. A. N. Fitch for instruction in the use of the modified Rietveld program.

References

1. P. D. Battle, T. C. Gibb, and S. Nixon, *J. Solid State Chem.* **79,** 75 (1989).
2. J. C. Grenier, J. Darriet, M. Pouchard, and P. Hagenmuller, *Mater. Res. Bull.* **11,** 1219 (1976).
3. J. C. Grenier, F. Menil, M. Pouchard, and P. Hagenmuller, *Mater. Res. Bull.* **12,** 79 (1977).
4. M. A. Alario-Franco, M. J. R. Henche, M.

Vallet, J. M. G. Calbet, J. C. Grenier, A. Wattiaux, and P. Hagenmuller, *J. Solid State Chem.* **46,** 23 (1983).

5. N. Nguyen, Y. Calage, F. Varret, G. Ferey, V. Caignaert, M. Hervieu, and B. Raveau, *J. Solid State Chem.* **53,** 398 (1984).
6. J. Rodriguez-Carvajal, M. Vallet-Regi, and J. M. Gonzalez-Calbet, *Mater. Res. Bull.* **24,** 423 (1989).
7. H. M. Rietveld, *J. Appl. Crystallogr.* **2,** 65 (1969).
8. A. N. Fitch, J. K. Cockcroft, and A. D. Murray, unpublished work.
9. R. E. Watson and A. J. Freeman, *Acta Crystallogr.* **14,** 27 (1961).
10. R. X. Fischer, *J. Appl. Crystallogr.* **18,** 258 (1985).
11. P. D. Battle, T. C. Gibb and P. Lightfoot, *J. Solid State Chem.* **76,** 334 (1988).
12. C. Greaves, A. J. Jacobson, B. C. Tofield, and B. E. F. Fender, *Acta Crystallogr. B* **31,** 641 (1975).